

Adsorption Mechanism of High-Concentration of Ammonium onto Chinese Natural Zeolite by Experimental Optimization and Theoretical Computation

Pan Liu

Xi'an University of Architecture and Technology School of Environmental and Municipal Engineering; Xi'an Aeronautical Polytechnic Institute

Yongjun Liu (✉ liuyongjun@xauat.edu.cn)

Xi'an University of Architecture and Technology <https://orcid.org/0000-0002-0411-5150>

Aining Zhang

Xi'an University of Architecture and Technology

Zhe Liu

Xi'an University of Architecture and Technology

Xingshe Liu

Xi'an University of Architecture and Technology

Lu Yang

Xi'an University of Architecture and Technology

Research

Keywords: Adsorption mechanism, Ammonium, Natural zeolite, Molecular Dynamics simulation

Posted Date: October 28th, 2021

DOI: <https://doi.org/10.21203/rs.3.rs-936615/v1>

License:   This work is licensed under a Creative Commons Attribution 4.0 International License. [Read Full License](#)

Abstract

Background

Natural zeolite, abundant hierarchically porous structure aluminosilicate mineral, have high affinity to ammonium in solution. A considerable amount of literature has been published on the removal of ammonium in waters by zeolite, but mainly focused on the low-content and even trace ammonium. Few literatures were reported about the natural zeolite as adsorbent to remove high-level of ammonium in coal chemical wastewater. Therefore, adsorption mechanism of high-concentration ammonium in aqueous solution using Chinese natural zeolite was disclosed by the strategy of experimental optimization combining with Molecular Dynamics simulation.

Results

The natural zeolite presented unique adsorption performances for high- ammonium distinguish from that of low ammonium, which were characterized as exhibiting faster adsorption rate, greater loading capacity and apparent desorption. The hybrid physical-chemical adsorption as the mechanism was induced from the adsorption kinetics and isotherm study in 4000 mg-N/L solution. Besides to the electrostatic attraction between the framework and guest ammonium exchanged by metal cations in the zeolite framework, the existence of the chemical bonding and hydrogen bonding forces was supported experimentally from the ion exchange capacity (IEC) investigation by the great disequilibrium between the total exchanged metal cations and ammonium. Moreover, the above were confirmed theoretically by the calculated results in the perspective of bonding strength in MD simulation. Considering comprehensively, we concluded physisorption dominated the initial adsorption stage as multilayer adsorption and chemisorption governed the subsequent adsorption process as monolayer form. Besides, the putative explanation for the desorption-occurrence was given that most ammonium concentrated in the channel openings physically, and transferred into the bulk solution preferentially through the mesopores and macropores.

Conclusions

Overall, we have demonstrated that the Chinese natural zeolite had the potential to capture high-concentration ammonium in wastewater remediation effectively. Considering with several research thinking comprehensively, this investigation enriched the adsorption mechanism research, and provided a novel insight for designing a workable approach for rapidly alleviating subsequent water decontamination processes using low-cost abundant minerals.

Highlights

- High-concentration ammonium (4000 mg /L) was removed by the Chinese natural zeolite.
- Adsorption mechanism of high-concentration ammonium was investigated.
- Hybrid physisorption and chemisorption as the mechanism were responsible for the efficient adsorption of ammonium.
- Physisorption dominated the initial adsorption stage as multilayer adsorption while chemisorption governed the later process as monolayer form.

1 Background

Natural zeolites are crystalline hydrated aluminosilicate minerals with abundant pores filled with alkali, alkaline earth cations and water and have valuable physicochemical properties like unique selective sorption, ion exchange and thermal stability. Natural zeolites have been used broadly for wastewater treatment [1–7].

Previous studies have mainly focused on the application of natural, modified, and synthetic zeolites for the removal of low-concentration (< 200 mg-N/L) and trace ammonium in municipal sewage, groundwater, or tap water [8–11]. However, high-concentration ammonium removal using natural zeolite are rarely researched. Generally, air stripping method is adopted for high ammonium removal [12, 13]. However, air stripping usually requires an elevated alkalinity and temperature to increase the proportion of gaseous NH_3 and continuously adds acid to reduce the alkalinity before discharge, which pollutes the atmosphere seriously and increases the operating cost. Compared to other techniques, adsorption technique has many favorable adsorption characteristics, like high affinity towards ammonium, low-cost, convenience for engineering configurations as well as environmental friendliness[14]. In addition, natural zeolites are available in abundance. These advantages make it competitive to remove of high-concentration ammonium using natural zeolite environmentally.

Numerous literatures investigated the adsorption mechanisms of ammonium removal, but almost all of them focused on the low-concentration ammonium removal. The adsorption mechanisms were studied primarily on the basis of the adsorption kinetics, isotherm and thermodynamics analysis, and the final conclusions were drawn from the following aspects. Generally, the rate-limiting step in the adsorption process from the adsorption kinetics analysis was determined from the hypothesis and the representative significance of each parameter of the best-fitted one from the pseudo-first-order, pseudo-second-order, intraparticle diffusion and/or Elovich model or others which had the higher value of the coefficient of determination (R^2)[8, 9, 15, 16]. Then, the adsorption form can be deduced from the results of the adsorption isotherm, such as monolayer is considered if Langmuir model fitted the experimental data, and multilayer if the Freundlich fitted better[17, 18]. Undoubtedly, other complicated models with more parameters were also chosen to explore the absorptive mechanism more accurately[18]. Further, the type of interaction force, e. g. physical adsorption or chemical adsorption, was established synthetically based on the results of adsorption kinetics, equilibrium and the thermodynamic investigation[9, 19]. The different interaction implied different adsorption strength between adsorbent and adsorbate[18]. In conclusion, the adsorption mechanism was depicted as the ion exchange, electrostatic attraction, chemisorption, or formation of complexes[17–20].

The adsorption efficiency of a specific adsorption process is influenced by many factors. Accordingly, researches on the adsorption mechanism should not only limit to the establishments of the adsorbate's mass-transferring process and their interaction forces, which are undoubtedly vital and indispensable in the adsorption process. Fundamentally, the characteristics of mass-transferring and adsorption process are greatly affected by the physicochemical properties of adsorbents and adsorbates together with the nonnegligible operating conditions. The effects of zeolites' framework on ammonium adsorption have been reported largely in previous studies, and the most focused on the influences of the structural features such as the surface area, particle size and surface chemistry of the adsorbents on the removal of cationic substances[18, 21, 22]. However, the effects of these factors on high-concentration ammonium were less reported. In 2013, L. Lin et al found that ion exchange was the dominant ammonium adsorption mechanism, but the order of exchange selectivity was different in different ammonium solutions ($10 \sim 4000$ mg-N/L) with Na^+ as the predominant ions for ammonium at low concentrations while Ca^{2+} exceeding Na^+ at high ammonium levels (≥ 1000 mg-N/L)[20]. This shows that the adsorption behaviors of zeolites in different-level ammonium solutions are different, however, the adsorption mechanism at high concentrations was not explored further in this study. M. J. Manto et al investigated the ammonium recovery in 1000mg-N/L aqueous solution using ZSM-5 as sorbent, and observed that the uptake of ammonium was much higher than the cation exchangeable capacity (CEC) on the ZSM-5[23]. The formation of hydrogen bonding between ammonium and the framework oxygen might cause excess capacity than CEC [24]. Both Lin Ye et al and O'Connor et al. groups revealed the multiple hydrogen bonding between the guest ammonium and oxygen atoms were formed in the Molecular Dynamics (MD) simulation of zeolites ammonium capture [24, 25]. These results mean great potentialities of the hybrid multiple interactions and has necessity to further investigate the complex ammonium adsorption mechanism for high-concentration ammonium by zeolite.

Based on the above considerations, the major purpose of the current study was to investigate of the adsorption mechanism of high-concentration ammonium (1000 ~ 4000 mg-N/L) using Chinese natural zeolite with the strategy of experimental research and Molecular Dynamics simulation. The research contents were in the following aspects: 1) to systematically investigate adsorption characteristics including the effects of various testing parameters such as natural zeolite dosage, operational temperature, and initial ammonium concentration on ammonium removal in natural zeolite adsorption process; 2) to explore the adsorption mechanism of high-concentration ammonium onto natural zeolite from the adsorption kinetic and equilibrium studies; 3) to identify the interaction forces between ammonium and zeolite framework through MD simulation; 4) to propose the possible mechanism for the enhancement of ammonium removal performance over natural zeolite; 5) to put forward our future outlook. This investigation enriched the adsorption mechanism for ammonium removal, and provided a novel insight for designing a feasible approach for rapid reduction of high concentration ammonium using low-cost abundant minerals and alleviating subsequent water decontamination processes.

2 Experimental Sections

2.1 Materials

The Chinese natural zeolite from Zhengzhou in Henan Province of China was ground into particles with the size ranging from 0.5-1.0 mm. Before being used for batch experiments, the zeolite particles were rinsed with deionized water and dried in an oven at 105°C overnight. Analytical reagent grade ammonium chloride and sodium chloride were purchased from Tianjin chemical reagent Co., Ltd.

2.2 Characterization techniques

The morphology of natural zeolite was characterized by SEM (ZEISS MERLIN, Germany), the chemical composition was characterized by Energy Dispersion X-ray Spectrometry (EDS, Bruker, USA), and the mineral species were characterized by an X-ray diffractometer (XRD, Rigaku Ultimate IV, Japan). The specific surface area, pore volume, and pore size distribution of natural zeolite were measured by the N₂ adsorption-desorption experiment with a heating rate of 10°C/min at 77 K using an Automatic Volumetric Sorption Analyzer (ASAP2460, TSI, America).

2.3 Liquid-phase adsorption experiments

Firstly, 5 g Chinese natural zeolite and 100 mL NH₄Cl solution with a prescribed initial concentration (1000 ~ 4000 mg-N/L) without pH adjustment were placed in a 250 mL Erlenmeyer flask and stirred at a specified temperature in the thermostatic shaker (HZQ-X3000, China) for several hours. Then the suspension after adsorption was filtered via a 0.22-μm filter and the filtrate was analyzed for the residual ammonium concentration with Nessler's reagent spectrophotometry method at 420 nm with a Hitachi UV/visible spectrophotometer (U-2001).

2.4 Simulation of zeolite ammonium capture and bonding strength

In this study, the interaction between a rigid ammonium ion and zeolite framework was our focused objective. All the structures (zeolite substrate, ammonium ion and water molecule) were determined with Density Functional Theory (DFT) method using the Dmol³ program package in Materials Studio 2018, and the initial zeolite structure as shown in **Figure 1A** was used to model the geometry of the framework. The exchange and correlation effect were described by using Perdew-Burke-Ernzerhof (PBE) functional[26], within a generalized gradient approximation (GGA) approach. Subsequently, the Hirshfeld charge analysis of the optimized structures was carried out, and these stable charged structures were applied to dynamics simulation using the Forcite module.

The high-ammonium solution model was built with the Amorphous Cell module, and the initial cubic simulation lattice of the system was $x = 39.17 \text{ \AA}$, $y = 39.96 \text{ \AA}$, and $z = 240 \text{ \AA}$. There was a 2-nm-high vacuum layer on the top of the solution to weaken the effect of zeolite substrate in the upper periodic lattice, as shown in **Figure 1B**. The simple point charge (SPC) model[27], describing the water solution environment accurately [28], was employed for all water molecules. All molecular dynamics simulations were performed in the COMPASS force field[29, 30] and equilibrated at constant temperature (308.15 K) and with the volume (NVT) of 10 ns.

3 Results And Discussion

3.1 Characterization of Chinese natural zeolite

The Chinese natural zeolite was detected by XRD to confirm the mineral species and their contents were obtained with the Rietveld method. As revealed in Figure 2A, the chosen zeolite is rich in heulandite (w.t. 57.43%) besides sanidine, tridymite and quartz. The morphologies of the natural zeolite was observed by SEM. As shown in Figure 2B, the zeolite presented the lamellar structure with large pores at the intersections the slices of different orientations, which was characterized by geometrically well-defined channels and cavities, and largely govern the mobility and siting of interstitial ions and their availability for exchanges.

The typical type IV isotherm with a fairly clear plateau was observed from N₂ adsorption-desorption isotherm by the BJH pore size analysis (Figure 2C). The desorption curve shown an extensive range of mesopore structure and could be attributed to plate-like particles with slit-shaped pores[31]. The conclusion was supported by the results of pore size distribution as shown in Figure 2D that abundant mesopores dominated the zeolite skeleton structure and some microporous together with few macropores presented. The total pore volume of zeolite was also not large enough ($V_p = 0.059 \text{ cm}^3/\text{g}$), however, its adsorption capacity was much higher than some reported zeolites (**Table 1**). The low Si/Al ratio of 4.51 in the framework of the chosen natural zeolite determined by EDS (Table 2), indicated the selected zeolite had great affinities for ammonium ions. Besides, the natural zeolite was rich in K metal cation as illustrated in **Table 2**.

3.2 Adsorption characteristics of Chinese natural zeolite

3.2.1 Adsorption performances

The effect of various treatment processes on the high concentration ammonium removal was assessed systematically in order to evaluate the effect of natural zeolite in adsorption process (**Figure 3**). Comprehensively considering the energy-consumption, environmental-friendly requirements and other factors, the optimal experiment was carried out with zeolite dosage of 5 g/100 mL at an optimal temperature of 35°C for different initial ammonium concentrations (100 ~ 4000 mg-N/L) in an aqueous medium without adjusting pH.

Table 2
Chemical compositions of the Chinese natural zeolites by EDS.

| Chemical elements | wt.% | Chemical elements | wt.% |
|-------------------|-------|-------------------|------|
| O | 47.12 | Fe | 1.40 |
| Si | 26.87 | Na | 0.82 |
| Al | 5.72 | Ca | 0.77 |
| K | 2.76 | Mg | 0.34 |
| others | 14.2 | | |

As illustrated in **Figure 3C, 3D**, the adsorption characteristics of natural zeolite on high-concentration ammonium were significantly distinctive from that on low-concentration ammonium (<1000 mg-N/L). The adsorption behaviors for low ammonium in our investigation were consistent with the reported that definite adsorption capacities were eventually maintained when adsorption was in equilibrium[32–34]. The adsorption rate and capacity for ammonium were both enhanced when the initial concentration was increased. Excellent loading capacity of 22.72 mg/g was obtained even within first 10 min in 4000 mg-N/L solution. Subsequently, the overall capacity increased to the maximum 29.48 mg/g. Based on the related review [35], ammonium adsorption capacity onto natural zeolite was generally 2.7~30.6 mg/g, indicating that the Chinese natural zeolite had an excellent adsorption capacity for ammonium. This inference was also supported by a set of comparative result with their adsorption capacities of other natural and modified zeolites (Table 3).

Table 3
Adsorption characteristics for ammonium by the selected Chinese natural zeolite and other reported materials.

| Samples | C_0 (mg/L) | Equilibrium time (min) | Q_{max} (mg/g) | Reference |
|----------------------------------|--------------|------------------------|------------------|------------|
| natural zeolite | 1000 ~ 4000 | 180 | 29.48 | this study |
| Iranian zeolite | 90 ~ 3610 | 60 | 11.5 | [18] |
| natural Chinese (Chende) zeolite | 50 ~ 300 | 180 | 9.41 | [16] |
| Na-Yemeni natural zeolite | 10 ~ 250 | 20 | 11.2 | [19] |
| Modified bentonite | 0 ~ 350 | 60 | 5.85 | [36] |

Obvious desorption phenomenon was also reflected in **Figure 3C** when the ammonium concentration was above 3000 mg-N/L, and it became more notable as ammonium capture process continued in 4000 mg-N/L solution. The desorption occurred mainly at the initial adsorption stage as illustrated in **Figure 3C**. A significant decrease of loading capacity to 18.82 mg/g was observed at 30 min in 4000 mg-N/L solution, which was still higher than that of other zeolites at 3 h or even longer adsorption time[32, 34]. The concomitant desorption was explained from the perspective of the adsorbent's characterization together with the zeolite–ammonium interactions. At early stage of ammonium capture, plenty of ammonium ions rushed into the pores and concentrated in the openings of the pore networks in natural zeolite by some weak interactions except for electrostatic attraction. Release ammonium into the bulk solution from the openings of the meso- and macropores took priority to diffuse toward internal pores and cavities of the skeleton, then the corresponding desorption occurred. On the consideration of adsorbent-adsorbate interaction, weak physical interaction forces also existed. In fact, multiple hydrogen bonds between the adsorbed ammonium hydrogen

and framework oxygen atoms of natural zeolite presented, and the hydrogen bonding effect was responsible for the observed desorption phenomenon. The detailed proof of physical interactions will present in the MD simulation part.

3.2.2 Ion exchange capacity for ammonium

The ammonium ion exchange selectivity for metal cations in the framework was investigated in the 4000 mg-N/L solution. Assuming that the exchangeable cations in zeolite were Na^+ , K^+ , Ca^{2+} and Mg^{2+} [37], the content of exchanged different metal cations at different adsorption time was monitored using atomic absorption spectrometry and the result was shown in **Figure 4A**. As seen in **Figure 4A**, the ammonium ion exchange selectivity for metal cations onto the natural zeolite followed the order of $\text{Ca}^{2+} > \text{Na}^+ > \text{K}^+ > \text{Mg}^{2+}$ at first 3 h, which was distinguished from $\text{Na}^+ > \text{K}^+ > \text{Ca}^{2+} > \text{Mg}^{2+}$ observed by Watanabe et al. [38]. This inconsistency was attributed to the difference in chemical compositions of their zeolites containing rather low Ca content, and the low initial ammonium concentration (below 500 mg-N/L). However, Lin et al. have also found that Ca^{2+} started to dominate the ion exchange process when the initial ammonium concentration was increased to above 1000 mg-N/L [20], indicating that the ion exchange selectivity of high-concentration ammonium was completely distinguish from that in low- ammonium solution. Subsequently, the released Na^+ and K^+ increased greatly after exchangeable Ca^{2+} ions were exhausted, and the order changed to $\text{Na}^+ > \text{K}^+ > \text{Ca}^{2+} > \text{Mg}^{2+}$. The interpretation for slight decrease of soluble Ca^{2+} concentration was that the released Ca^{2+} was re-exchanged to zeolite with Na^+ and K^+ because of the strong affinity of Ca^{2+} for the zeolite framework. The low content in zeolite and high hydrated radius in the solution hindered the exchange of Fe^{2+} and Mg^{2+} with ammonium ions [39].

If only the strong electrostatic attraction was responsible for high capacity of ammonium because of the low ratio of Si/Al in the natural zeolite skeleton, the total loading ammonium capacity on zeolite should equalize the sum of exchanged cations. The sum of exchanged cations is defined as the ion exchange capacity (IEC) and expresses as follow formula:

$$\text{IEC} = [\text{Na}^+] + [\text{K}^+] + 2 [\text{Ca}^{2+}] + 2 [\text{Mg}^{2+}] = [\text{NH}_4^+]$$

The calculated IEC was compared with the total reduced ammonium concentration and plotted in **Figure 4B**. **Figure 4B** shown that the ammonium ions adsorption capacity was much higher than the actual IEC at any time interval, demonstrating other interacting forces coexisted with electrostatic attraction and took greater responsibility for efficient ammonium removal. The existence of other interactions will be supported by the conclusions of adsorption kinetics, equilibrium and MD simulation.

Table 4
Theoretical parameters and error values associated with kinetic models.

| C_0 (mg/g) | Pseudo first-order | | | | Pseudo second-order | | | | Elovich | | | |
|-----------------|--------------------|--------|-------|----------|---------------------|--------|-------|----------|---------------------|---------|-------|----------|
| | q_e | k_1 | R^2 | χ^2 | q_e | k_2 | R^2 | χ^2 | α | β | R^2 | χ^2 |
| 1000 | 9.99 | 0.077 | 0.41 | 0.24 | 10.28 | 0.018 | 0.86 | 0.071 | 1263.32 | 1.28 | 0.78 | 0.35 |
| 2000 | 15.18 | 0.061 | 0.45 | 0.72 | 15.70 | 0.0085 | 0.89 | 0.21 | 368.85 | 0.73 | 0.70 | 1.59 |
| 3000 | 18.06 | 0.0053 | 0.32 | 0.56 | 18.38 | 0.016 | 0.80 | 0.16 | 82623.66 | 0.93 | 0.39 | 3.56 |
| 4000 | 24.89 | 0.11 | 0.25 | 0.77 | 25.17 | 0.016 | 0.75 | 0.18 | 7.414×10^6 | 0.86 | 0.32 | 5.72 |

3.3 Adsorption kinetics and isotherm properties

3.3.1 Adsorption kinetics

To investigate the kinetic properties of natural zeolite-ammonium adsorption system, pseudo-first-order, pseudo-second-order and Elovich model were evaluated by the nonlinear fitting with the experimental data and their expressions were listed in **Table S1**. Considering the obtained results of the correlation coefficient (R^2) and Chi-square values (χ^2), the adsorption for ammonium followed the pseudo-second-order model (**Figure 5, Table 4**). The pseudo-second-order model presumes reactions with more chemical affinity between ammonium ions and zeolite surfaces[40, 41].

The thermodynamic parameters related to the adsorption process, i.e., Gibb's free energy change (ΔG^0 , $\text{kJ}\cdot\text{mol}^{-1}$), enthalpy change (ΔH^0 , $\text{kJ}\cdot\text{mol}^{-1}$) and entropy change (ΔS^0 , $\text{J}\cdot\text{mol}^{-1}\cdot\text{K}^{-1}$) were also calculated according to equations in **Table S1** based on the adsorption equilibrium at different temperatures, as shown in Table 5 and **Figure 6**. Negative ΔG^0 and the positive ΔH^0 suggested that the adsorption for ammonium was spontaneous and endothermic.

3.3.2 Adsorption Isotherm

The adsorption equilibria properties of natural zeolite for ammonium ions were assessed with the results of the nonlinear fitting with Langmuir model, Freundlich model and Redlich-Peterson model (**Figure 7**). The illustrative equations of the inspected models were documented in **Table S1** and the isotherm parameters were presented in **Table 6**. The Langmuir model hypothesizes homogeneous and monolayer adsorption of ammonium by natural zeolite while the Freundlich model presumes heterogeneous and multilayer uptake[42, 43]. Considering the values of χ^2 and R^2 , the adsorption result of ammonium by natural zeolite was consistent with Langmuir and Freundlich model with a preference for the Langmuir model as the fitting result was of lower χ^2 value (**Figure 7, Table 6**).

Langmuir isotherm dimensionless equilibrium parameter R_L was determined based on the equation listed in **Table S1**. $R_L > 1$, $0 < R_L < 1$, $R_L = 1$, and $R_L < 0$ implies unfavorable, favorable, linear, and irreversible adsorption, respectively[44–46]. In this study, $R_L = 0.15$, indicated favorable ammonium adsorption at the given experiment conditions (Table 6). Freundlich model as also fitted with the experimental data for the natural zeolite. Freundlich constant 'n' represents the intensity of cation exchange and $n > 1$ indicates higher intensity and favorability for chemisorption[46–48]. In our investigation, $n = 1.92$ suggested, chemisorption was one of the dominant adsorption mechanisms of natural zeolite for ammonium (Table 6). Besides, the theoretical maximum adsorption capacity was 31.88 mg/g from the Langmuir model (Table 6), very close to the actual loading capacity of 29.48 mg/g (Table 3),

demonstrating this selected zeolite had great affinities to ammonium ions. On the other hand, excellent adsorption capacity was confirmed equally by comparing with other natural and modified zeolites in previous studies as summarized in Table 3.

3.4 Simulation of zeolite ammonium capture and bonding strength

This work provided a detailed investigation of zeolite–adsorbent interactions via MD simulation. O, Si and Al atoms of the zeolite framework were all considered as the possible adsorption sites for ammonium capture (**Figure S1**). The isomorphous substitution of aluminum atoms to silicon results in insufficient positive charges in the crystal lattice, which was compensated by exchangeable cations in the intrinsic pore networks throughout the aluminosilicate crystallites. The existing of excessive net negative charges means some O atoms of the framework existed as the unbonded form, unlike the bridged Al-O-Si pattern. Therefore, both the bridged and unbonded O atoms were considered as the independent site and performed the corresponding calculations respectively.

Representation of the random position of ammonium on pore surface was depicted in **Figure 1C**, the detail shown bonded ammonium to zeolite framework. The wide extent of the distances between ammonium and framework

oxygens was divided into two distance ranges which inferred as two types of interactions respectively according to the distance division of H-bonds in all intermolecular N-H...O/O-H...N by G. Gilli et al[49]. The distance of 2.746 ~ 2.974 Å suggested the existence of weak hydrogen bonds while the range of 2.090 ~ 2.522 Å (**Figure 8**) was attributed to strong covalent linkage because the distance

Table 5
The calculated thermodynamic parameters.

| Temperature (K) | ΔG^0 (kJ/mol) | ΔH^0 (kJ/mol) | ΔS^0 (J/mol \cdot K) |
|-----------------|-----------------------|-----------------------|--------------------------------|
| 288 | -14.03 | 26.61 | 144.50 |
| 298 | -17.49 | | |
| 308 | -18.21 | | |
| 323 | -19.85 | | |
| 338 | -21.89 | | |

of the ammonium and framework oxygens was shortened by the electronic sharing between adsorbate and adsorbent. Therefore, the binding energy could expect to be high due to electron transfer from framework oxygen to bonded ammonium hydrogen atoms. The calculated adsorption energies between adsorbed ammonium and adsorption sites listed in Table 7 shown in detail that spontaneous adsorption occurred from the magnitude of the negative adsorption energies of every adsorption site. Moreover, the interaction between the ammonium hydrogen and framework oxygen atoms was the most stable, which was consistent with the reported by M. Khosravi et al[50]. With such high binding energy, one could expect to remove ammonium difficultly from the structure during zeolite regeneration, as tested in zeolite regeneration experiments (**Figure 9**). Only ~17% - ~32% release was observed dependent of the brine solution concentration, suggesting more ammonium were effectively trapped within the natural zeolite pore structure by strong acting forces.

The chemisorption of ammonium by natural zeolite represents the proceeding of electron transfer between bonded ammonium hydrogen and framework oxygen atoms [40, 41]. Hirshfeld charges of the adsorbed ammonium

Table 6
Different parameters and errors values associated with isotherm models.

| Isotherms model | Parameters | | | R ² | χ^2 |
|------------------|---------------|----------------|--------------|----------------|----------|
| Langmuir | $Q_m = 31.88$ | $K_L = 0.0014$ | $R_L = 0.15$ | 0.98 | 0.62 |
| Freundlich | $K_F = 0.41$ | $1/n = 0.52$ | $n = 1.92$ | 0.98 | 0.82 |
| Redlich-Peterson | $a = 0.80$ | $b = 1.36$ | $n = 0.53$ | 0.96 | 2.48 |

Table 7
The adsorption energy of ammonium on the four possible adsorption sites in zeolite.

| System | Bridged O site | Unbonded O site | Si site | Al site |
|-------------------------|----------------|-----------------|---------|---------|
| $E_{ads, cal}$ (kJ/mol) | -86.77 | -136.77 | -40.90 | -61.32 |

on framework bridged and unbonded oxygen sites were +0.433e and +0.378e respectively (**Figure 10**), suggesting a stronger electron transfer tendency from unbonded O atom to adsorbed ammonium. Therefore, these unbonded oxygen atoms had the greatest preference for chemisorption of ammonium ions onto zeolite surface.

3.5 Mechanism elucidation in ammonium adsorption process

In summary, from the adsorbent's characterization together with the adsorption studies and MD simulation it was verified that high-concentration ammonium adsorption mechanism onto Chinese natural zeolite contained both physical and chemical interactions according to the adsorption sequence. Therefore, considering the adsorption behaviors observed in the ammonium-zeolite system the main interactions responsible for high-concentration ammonium adsorption onto natural zeolite are elucidated in a diagrammatic illustration as shown in **Figure 11**.

The physisorption dominated the ammonium adsorption process in the initial adsorption stage as multilayer adsorption behavior, mainly the electrostatic interactions between the framework oxygen atoms and adsorbed ammonium ions as well as hydrogen bonding between the adsorbed ammonium hydrogen and framework oxygen atoms. In addition, because plenty of ammonium ions rushed preferentially into the openings of the pore networks in natural zeolite, ammonium release into the bulk solution from the openings of the meso- and macropores was much easier and significant desorption phenomena was observed correspondingly.

The chemisorption mechanism began to govern the later adsorption process mainly in the monolayer behavior and, of course the synergetic ion exchange process and hydrogen bonding were equally nonnegligible factors for accelerating ammonium capture. The excessive adsorption capacity beyond the equivalent of the total exchangeable metal cations and difficulty of ammonium release were the contributions of the chemical bonding force. The release of the adsorbed ammonium was evaluated under the conditions that the saturated zeolite was isolated and then re-dispersed into 100 mL of NaCl solution for 3 h. As illustrated in **Figure 9**, only 17% ~ 32% release dependent on the brine solution concentration was observed, suggesting more ammonium were effectively trapped within the pores and cavities of natural zeolite. These results confirmed the dominance of chemisorption mechanism in turn.

3.6 Future outlook

Future work will focus on ammonium recovery and regeneration of the natural zeolites as previous tests confirmed undesired (**Figure 9**). We will also investigate the realistic application of zeolites for wastewater remediation as appreciable distinctions could be revealed between the performances displayed in laboratory synthetic solutions and in the presence of actual industry wastewater which contains non-characteristic variables such as competitive species, pH and organic substances during the ion exchange process. Furthermore, the potential for conversion of ammonium to more environment-friendly species via catalytic oxidation and other techniques

will be investigated. Moreover, direct use of zeolites saturated by ammonium ions may be another new strategy because zeolites have the significant roles in improving soil structure and water retention and simultaneously as sustained-release agents for providing nitrogen nutrients in green vegetation, especially important in drought region.

4 Conclusion

In this study, we provided a detailed mechanism investigation of zeolite – ammonium interactions via experimental investigation and MD simulation. The unique adsorption behavior of ammonium onto natural zeolite was firstly observed when the initial concentration of ammonium in the synthetic wastewater solution was above 1000 mg-N/L and the Chinese natural zeolite had excellent adsorption capacity for high-concentration ammonium. The physisorption and chemisorption coexisted in the high-concentration ammonium adsorption process, which was concluded from the adsorption kinetics and equilibrium study. The existence of the chemical bonding force and hydrogen bonding was

proved from the calculated results in MD simulation. Finally, we induced the adsorption mechanism on the basis of the comprehensive results of adsorption kinetics and isotherm properties and the MD simulation combining with the adsorption characteristics. We thought physisorption including electrostatic attraction forces and hydrogen bonding between zeolite and adsorbed ammonium ions via the ion-exchange process was the dominate mechanism in the initial adsorption stage, and the subsequent process was governed by chemisorption mechanism. Physical interactions caused the ammonium desorption easily, especially in the first 30 min when the most ammonium was adsorbed onto the channel openings and transferred into the bulk solution more conveniently through the mesopores and macropores. Irreversible chemical adsorption made the release of adsorbed ammonium ions very difficult when the natural zeolite was in saturated state, which was also confirmed by the ammonium release experiments where maximum 32% release rate was obtained in the concentrated brine solution. All integrated interactions prompted the adsorption capacity close to the theoretical value. At last, several research thinking was brought forward as our future work and also could be seen as a reference for conducting related works. Overall, we have demonstrated that the Chinese natural zeolite had the potential to capture high-concentration ammonium in wastewater remediation effectively, and this investigation enriched the ammonium adsorption mechanism and provided a novel insight for rapidly alleviating subsequent water decontamination processes by a feasible adsorption approach using low-cost abundant minerals.

Declarations

Acknowledgments

Additional support was kindly provided by the Scientific Compass Organization. We also would like to express our sincere thanks to the anonymous reviewers. Their insightful comments were helpful for improving the manuscript.

Authors' contributions

PL conceived the project, prepared, tested and wrote the manuscript. YL, PL and ZL reviewed and corrected the manuscript. AZ contributed with the Molecular Dynamics simulation analysis. ZL and LY conceived the idea and contributed to the writing of the manuscript. All authors reviewed the manuscript. All authors read and approved the final manuscript.

Funding

The authors acknowledge financial support from National Natural Science Foundation of China (Grant No. 51978559) and the Key research and development project of Shaanxi province (Grant No. 2019ZDLSF05-06).

Availability of data and materials

The datasets used and/or analyzed during the current study are available from the corresponding author on reasonable request.

Ethics approval and consent to participate

Not applicable.

Consent for publication

Not applicable.

Competing interests

The authors declare that they have no competing interest.

References

1. Ates, A. (2018) Effect of alkali-treatment on the characteristics of natural zeolites with different compositions. *Journal of Colloid and Interface Science* 523: 266-281. <https://doi.org/10.1016/j.jcis.2018.03.115>
2. Hudcová, B. et al. (2021) Investigation of zinc binding properties onto natural and synthetic zeolites: Implications for soil remediation. *Microporous and Mesoporous Materials* 317: 111022. <https://doi.org/10.1016/j.micromeso.2021.111022>
3. Wang, H. et al. (2020) Purification mechanism of sewage from constructed wetlands with zeolite substrates: A review. *Journal of Cleaner Production* 258: 120760. <https://doi.org/10.1016/j.jclepro.2020.120760>
4. Valdés, H. et al. (2012) Natural zeolite reactivity towards ozone: the role of compensating cations. *Journal of Hazardous Materials* 227-228: 34-40. <https://doi.org/10.1016/j.jhazmat.2012.04.067>
5. Lin, L. et al. (2014) Ammonium assists orthophosphate removal from high-strength wastewaters by natural zeolite. *Separation and Purification Technology* 133: 351-356. <https://doi.org/10.1016/j.seppur.2014.07.010>
6. Valdés, H. et al. (2021) Removal of chlorinated volatile organic compounds onto natural and Cu-modified zeolite: The role of chemical surface characteristics in the adsorption mechanism. *Separation and Purification Technology* 258: 118080. <https://doi.org/10.1016/j.seppur.2020.118080>
7. Valdés, H. et al. (2014) Control of released volatile organic compounds from industrial facilities using natural and acid-treated mordenites: The role of acidic surface sites on the adsorption mechanism. *Chemical Engineering Journal* 244: 117-127. <https://doi.org/10.1016/j.cej.2014.01.044>
8. Guo, J. (2015) Adsorption characteristics and mechanisms of high-levels of ammonium from swine wastewater using natural and MgO modified zeolites. *Desalination and Water Treatment* 57 (12): 5452-5463. <https://doi.org/10.1080/19443994.2014.1003334>
9. Alshameri, A. et al. (2014) An investigation into the adsorption removal of ammonium by salt activated Chinese (Hulaodu) natural zeolite: Kinetics, isotherms, and thermodynamics. *Journal of the Taiwan Institute of Chemical Engineers* 45 (2): 554-564. <https://doi.org/10.1016/j.jtice.2013.05.008>
10. Tang, H. et al. (2020) Removal of Ammonium from Swine Wastewater Using Synthesized Zeolite from Fly Ash. *Sustainability* 12 (8): 3423. <https://doi.org/10.3390/su12083423>
11. Guaya, D. et al. (2015) Simultaneous phosphate and ammonium removal from aqueous solution by a hydrated aluminum oxide modified natural zeolite. *Chemical Engineering Journal* 271: 204-213. <https://doi.org/10.1016/j.cej.2015.03.003>
12. Zhang, L. et al. (2012) Ammonia stripping for enhanced biomethanization of piggery wastewater. *Journal of Hazardous Materials* 199-200: 36-42. <https://doi.org/10.1016/j.jhazmat.2011.10.049>
13. Yuan, M.-H. et al. (2016) Ammonia removal from ammonia-rich wastewater by air stripping using a rotating packed bed. *Process Safety and Environmental Protection* 102: 777-785. <https://doi.org/10.1016/j.psep.2016.06.021>
14. Huang, J. et al. (2018) Removing ammonium from water and wastewater using cost-effective adsorbents: A review. *J Environ Sci (China)* 63: 174-197. <https://doi.org/10.1016/j.jes.2017.09.009>
15. Abukhadra, M.R. et al. (2020) The effect of different green alkali modification processes on the clinoptilolite surface as adsorbent for ammonium ions; characterization and application. *Microporous and Mesoporous Materials* 300: 110145. <https://doi.org/10.1016/j.micromeso.2020.110145>
16. Huang, H. et al. (2010) Ammonium removal from aqueous solutions by using natural Chinese (Chende) zeolite as adsorbent. *Journal of Hazardous Materials* 175 (1-3): 247-52. <https://doi.org/10.1016/j.jhazmat.2009.09.156>

17. Alshameri, A. et al. (2018) Adsorption of ammonium by different natural clay minerals: Characterization, kinetics and adsorption isotherms. *Applied Clay Science* 159: 83-93. <https://doi.org/10.1016/j.clay.2017.11.007>
18. Malekian, R. et al. (2011) Ion-exchange process for ammonium removal and release using natural Iranian zeolite. *Applied Clay Science* 51 (3): 323-329. <https://doi.org/10.1016/j.clay.2010.12.020>
19. Alshameri, A. et al. (2014) The investigation into the ammonium removal performance of Yemeni natural zeolite: Modification, ion exchange mechanism, and thermodynamics. *Powder Technology* 258: 20-31. <https://doi.org/10.1016/j.powtec.2014.02.063>
20. Lin, L. et al. (2013) Adsorption mechanisms of high-levels of ammonium onto natural and NaCl-modified zeolites. *Separation and Purification Technology* 103: 15-20. <https://doi.org/10.1016/j.seppur.2012.10.005>
21. He Wenya, A.K., Ren Xiaoyan et al (2017) Inorganic layered ion-exchangers for decontamination of toxic metal ions in aquatic systems. *Journal of Materials Chemistry A* 5 (37): 19593-19606. <https://doi.org/10.1039/C7TA05076C>
22. Qiaorui Wang, C.Z., Zhenxing Shen, et al (2019) Polyethyleneimine and carbon disulfide co-modified alkaline lignin for removal of Pb^{2+} ions from water. *Chemical Engineering Journal* 359: 265-274. <https://doi.org/10.1016/j.cej.2018.11.130>
23. Manto, M.J. et al. (2018) Recovery of ammonium from aqueous solutions using ZSM-5. *Chemosphere* 198: 501-509. <https://doi.org/10.1016/j.chemosphere.2018.01.126>
24. Ye, L. et al. (2016) Probing atomic positions of adsorbed ammonia molecules in zeolite. *Chem Commun (Camb)* 52 (16): 3422-5. <https://doi.org/10.1039/c5cc10476a>
25. O'Connor, E. et al. (2020) Highly selective trace ammonium removal from dairy wastewater streams by aluminosilicate materials. *Journal of Industrial and Engineering Chemistry* 86: 39-46. <https://doi.org/10.1016/j.jiec.2019.10.027>
26. John P. Perdew, K.B., Matthias Ernzerhof (1996) Generalized Gradient Approximation Made Simple. *Physical Review Letters* 77: 3865-3868. <https://doi.org/10.1103/PhysRevLett.77.3865>
27. Straatsma, H.J.C.B.J.R.G.T.P.J. (1987) The missing term in effective pair potentials. *The Journal of Physical Chemistry* 91 (24): 6269-6271. <https://doi.org/10.1021/j100308a038>
28. Wiedemair, M.J. and Hofer, T.S. (2017) Towards a dissociative SPC-like water model-probing the impact of intramolecular Coulombic contributions. *Physical Chemistry Chemical Physics* 19 (47): 31910-31920. <https://doi.org/10.1039/c7cp06191a>
29. H. Sun, P.R., J. R. Fried (1998) The COMPASS force field: parameterization and validation for phosphazenes. *Computational and Theoretical Polymer Science* 8: 229-246. [https://doi.org/10.1016/S1089-3156\(98\)00042-7](https://doi.org/10.1016/S1089-3156(98)00042-7)
30. Sun, H. (1998) COMPASS: An ab initio force-field optimized for condensed-phase applications—overview with details on alkane and benzene compounds. *The Journal of Physical Chemistry B* 102: 7338-7364. <https://doi.org/10.1021/jp980939v>
31. Sing, K.S.W. (1985) Reporting physisorption data for gas-solid systems with special reference to the determination of surface area and porosity. *Pure and Applied Chemistry* 57 (4): 603-619. <https://doi.org/10.1351/pac198557040603>
32. Du, Q. et al. (2005) Ammonia removal from aqueous solution using natural Chinese clinoptilolite. *Separation and Purification Technology* 44 (3): 229-234. <https://doi.org/10.1016/j.seppur.2004.04.011>
33. Guo, X. et al. (2007) Removal of Ammonium from RO Permeate of Anaerobically Digested Wastewater by Natural Zeolite. *Separation Science and Technology* 42 (14): 3169-3185. <https://doi.org/10.1080/01496390701514949>

34. Wang, S. and Zhu, Z.H. (2006) Characterisation and environmental application of an Australian natural zeolite for basic dye removal from aqueous solution. *Journal of Hazardous Materials B136* (3): 946-52. <https://doi.org/10.1016/j.jhazmat.2006.01.038>
35. Wang, S. and Peng, Y. (2010) Natural zeolites as effective adsorbents in water and wastewater treatment. *Chemical Engineering Journal* 156 (1): 11-24. <https://doi.org/10.1016/j.cej.2009.10.029>
36. Cheng, H. et al. (2019) Adsorption of ammonia nitrogen in low temperature domestic wastewater by modification bentonite. *Journal of Cleaner Production* 233: 720-730. <https://doi.org/10.1016/j.jclepro.2019.06.079>
37. Inglezakis, V.J. (2005) The concept of "capacity" in zeolite ion-exchange systems. *Journal of Colloid and Interface Science* 281 (1): 68-79. <https://doi.org/10.1016/j.jcis.2004.08.082>
38. Watanabe, Y. et al. (2007) Ion Exchange Behavior of Natural Zeolites in Distilled Water, Hydrochloric Acid, and Ammonium Chloride Solution. *Separation Science and Technology* 38 (7): 1519-1532. <https://doi.org/10.1081/ss-120019090>
39. Kantiranis, N. et al. (2011) Extra-framework cation release from heulandite-type rich tuffs on exchange with NH_4^+ . *Journal of Environmental Management* 92 (6): 1569-76. <https://doi.org/10.1016/j.jenvman.2011.01.013>
40. Li, X. et al. (2018) Adsorption characteristics of Copper (II), Zinc (II) and Mercury (II) by four kinds of immobilized fungi residues. *Ecotoxicology and Environmental Safety* 147: 357-366. <https://doi.org/10.1016/j.ecoenv.2017.08.058>
41. A.I.A. Sherlala, A.A.A.R., M.M. Bello, A. Buthiyappan (2019) Adsorption of Cu(II), Ni(II) and Zn(II) Ions by Nano Kaolinite Thermodynamics and Kinetics Studies. *Journal of Environmental Management* 246: 547-556. <https://doi.org/10.5281/zenodo.2644985>
42. Munawar Iqbal, M.A., J. Nisar, et al (2019) Bioassays Based on Higher Plants As Excellent Dosimeters for Ecotoxicity Monitoring: A Review. *Chemistry International* 5 (1): 1-80. <https://doi.org/10.31221/osf.io/z2ynm>
43. Akl Awwad, M.A., Marwa Al-aqarbeh (2020) TiO_2 -Kaolinite Nanocomposite Prepared from the Jordanian Kaolin Clay Adsorption and Thermodynamics of Pb(II) and Cd(II) Ions in Aqueous Solution. *Chemistry International* 6 (4): 168-178. <https://doi.org/10.5281/zenodo.3597558>
44. Kizito, S. et al. (2015) Evaluation of slow pyrolyzed wood and rice husks biochar for adsorption of ammonium nitrogen from piggery manure anaerobic digestate slurry. *Science of the Total Environment* 505: 102-12. <https://doi.org/10.1016/j.scitotenv.2014.09.096>
45. Reguyal, F. et al. (2017) Synthesis of magnetic biochar from pine sawdust via oxidative hydrolysis of FeCl_2 for the removal sulfamethoxazole from aqueous solution. *Journal of Hazardous Materials* 321: 868-878. <https://doi.org/10.1016/j.jhazmat.2016.10.006>
46. Foo, K.Y. and Hameed, B.H. (2010) Insights into the modeling of adsorption isotherm systems. *Chemical Engineering Journal* 156 (1): 2-10. <https://doi.org/10.1016/j.cej.2009.09.013>
47. Mathurasa, L. and Damrongsiri, S. (2018) Low cost and easy rice husk modification to efficiently enhance ammonium and nitrate adsorption. *International Journal of Recycling of Organic Waste in Agriculture* 7 (2): 143-151. <https://doi.org/10.1007/s40093-018-0200-3>
48. Khalil, A. et al. (2018) Removal of ammonium from fish farms by biochar obtained from rice straw: Isotherm and kinetic studies for ammonium adsorption. *Adsorption Science & Technology* 36 (5-6): 1294-1309. <https://doi.org/10.1177/0263617418768944>
49. G. Gilli and Gilli, P. (2000) Towards an unified hydrogen-bond theory. *Journal of Molecular Structure* 552: 1-15.
50. Khosravi, M. et al. (2019) The Exchange Mechanism of Alkaline and Alkaline-Earth Ions in Zeolite N. *Molecules* 24 (20): 3652. <https://doi.org/10.3390/molecules24203652>

Tables

Table 1 is not available with this version.

Figures

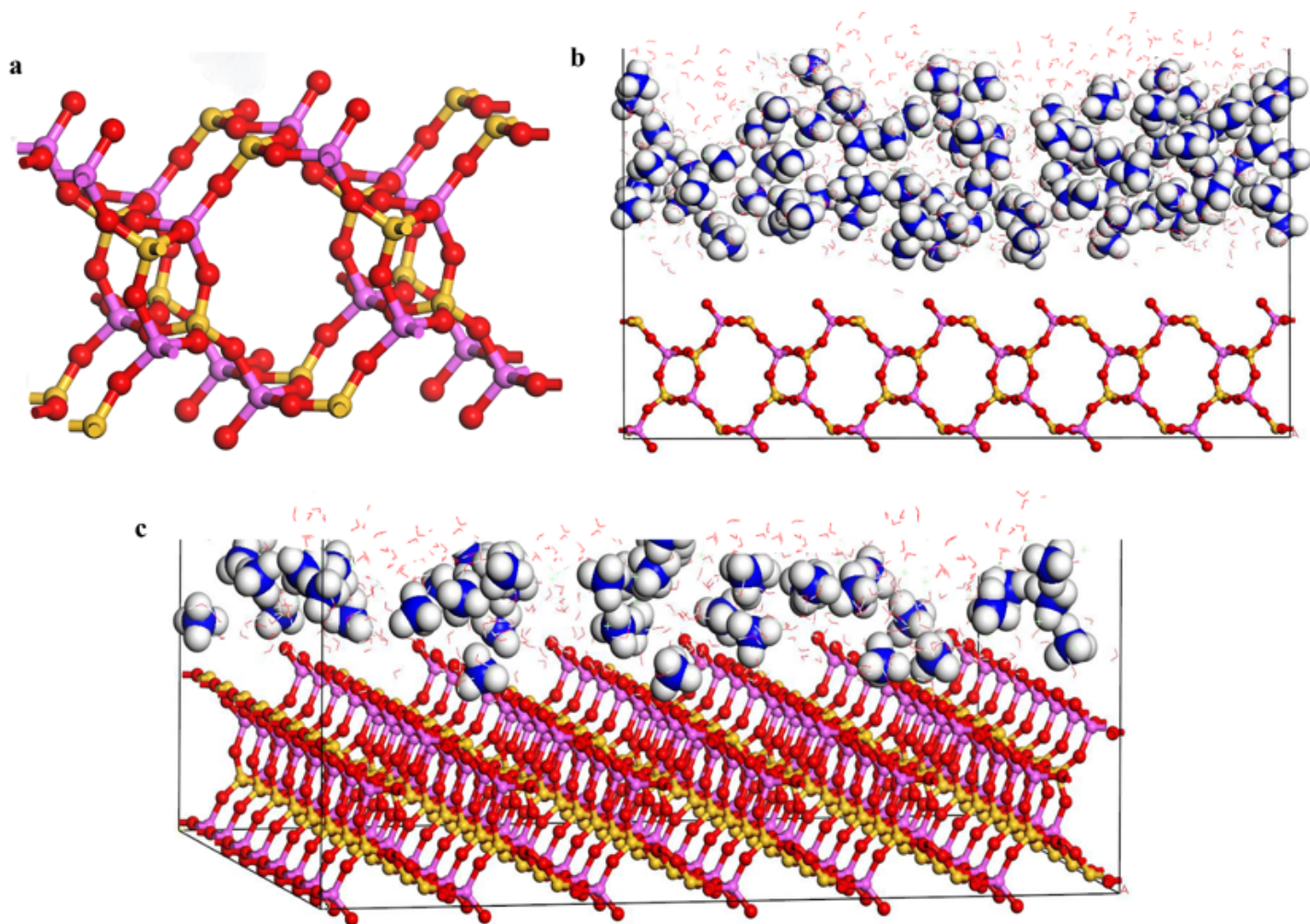


Figure 1

The optimized structures of high-ammonium adsorption onto the natural zeolite. (A) structure of the Chinese natural zeolite; (B) the initial model with 2-nm-high vacuum layer in the upper periodic lattice; (C) random position model of ammonium on zeolite surface. Yellow represents Si atoms, pink = Al, red = O, white= H, blue= N.

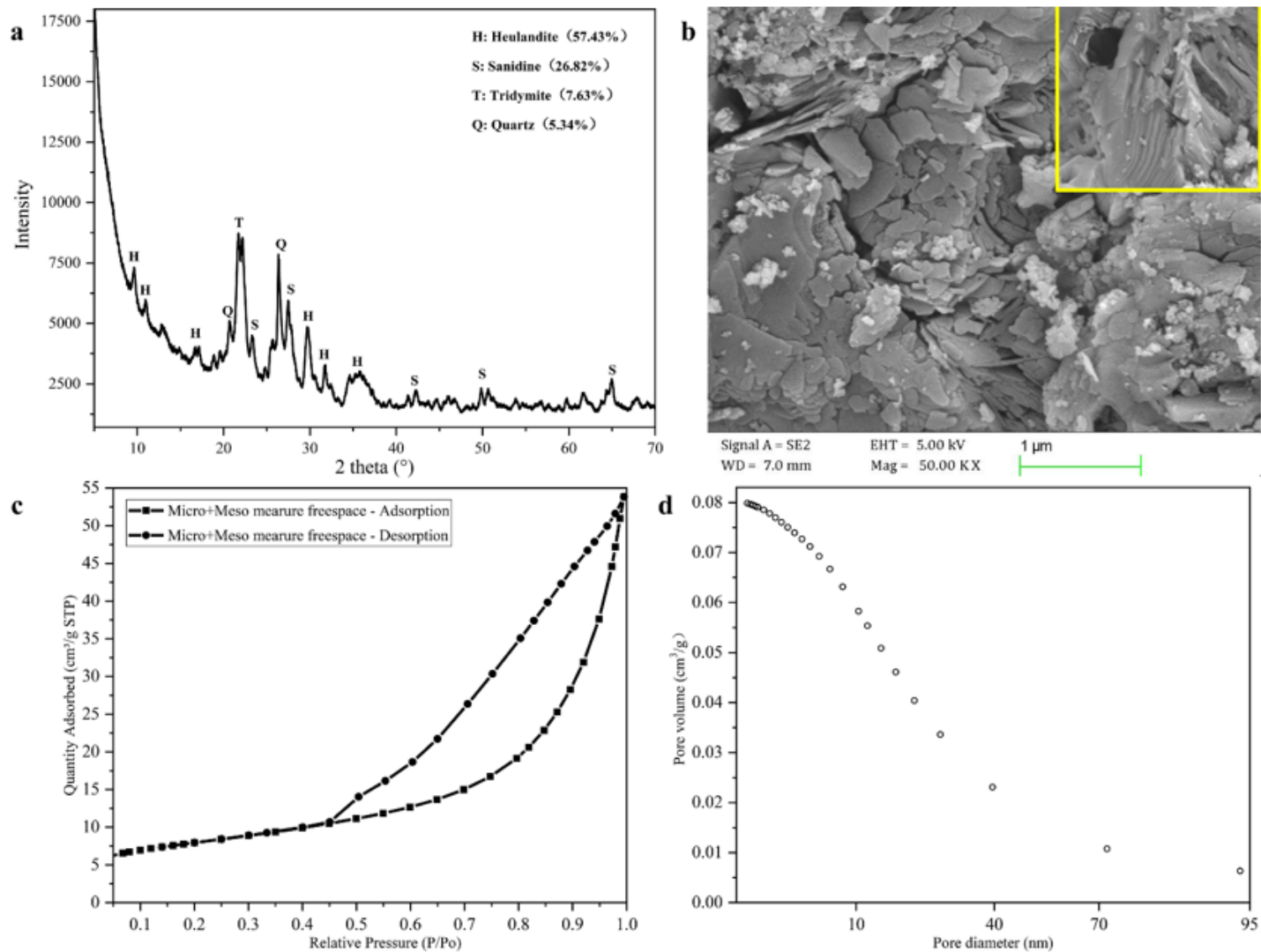


Figure 2

The basic properties of the natural zeolite: (A) XRD patterns; (B) SEM images; (C) N₂ adsorption-desorption isotherms at 77K; (D) corresponding BJH pore size distribution.

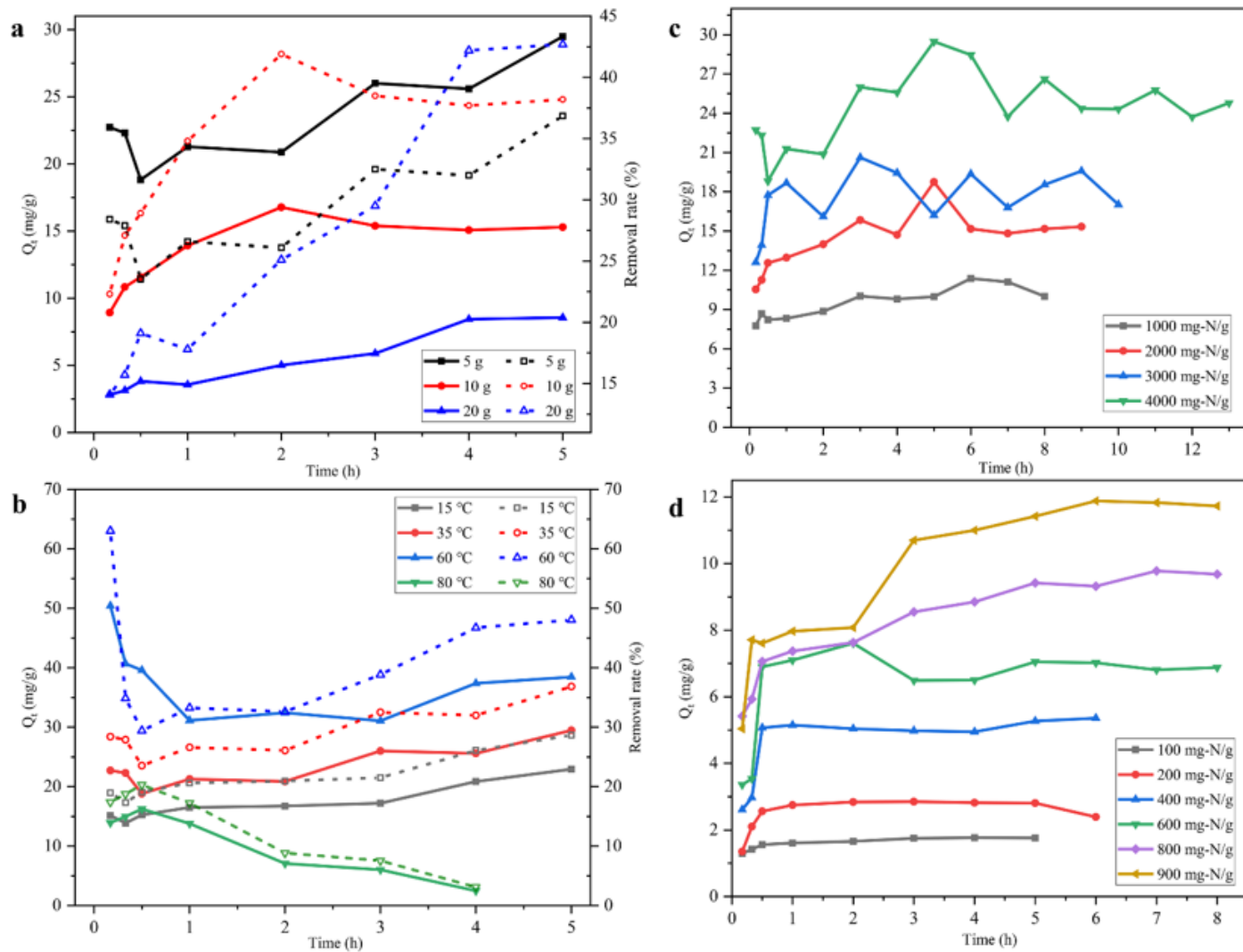


Figure 3

The effect of various treatment processes on the high concentration ammonium removal was evaluated.

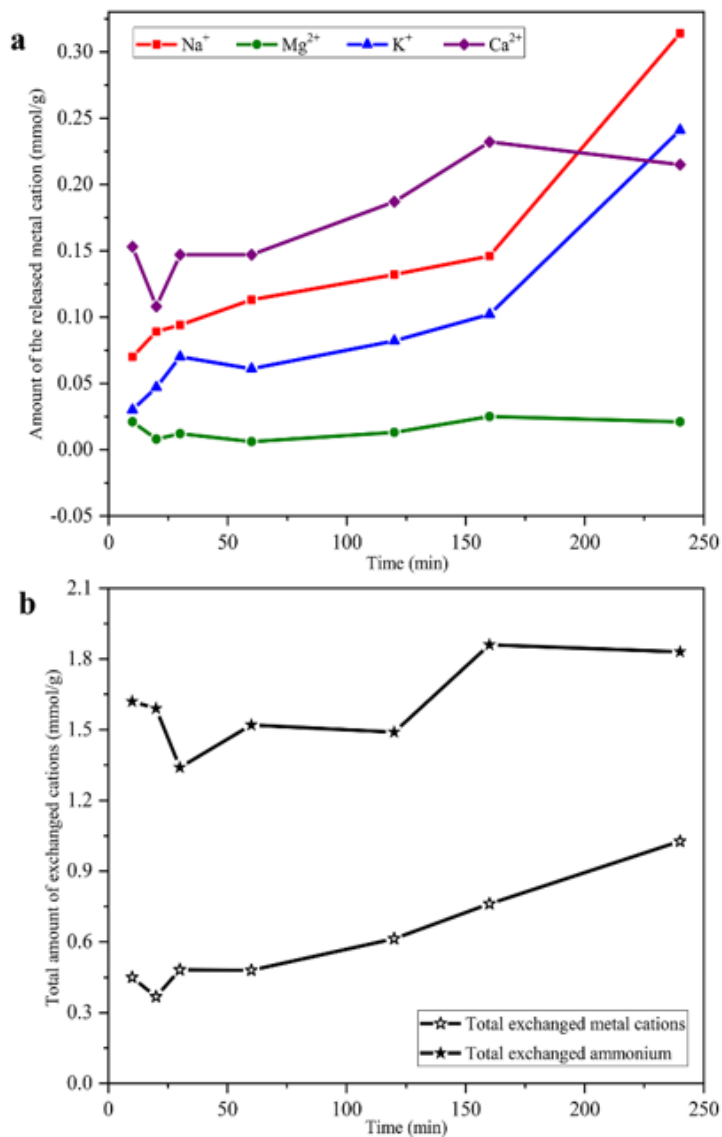


Figure 4

The exchange of the metal cations in natural zeolite and ammonium in solution. (A) the released metal cations; (B) the total exchanged ammonium and metal cations.

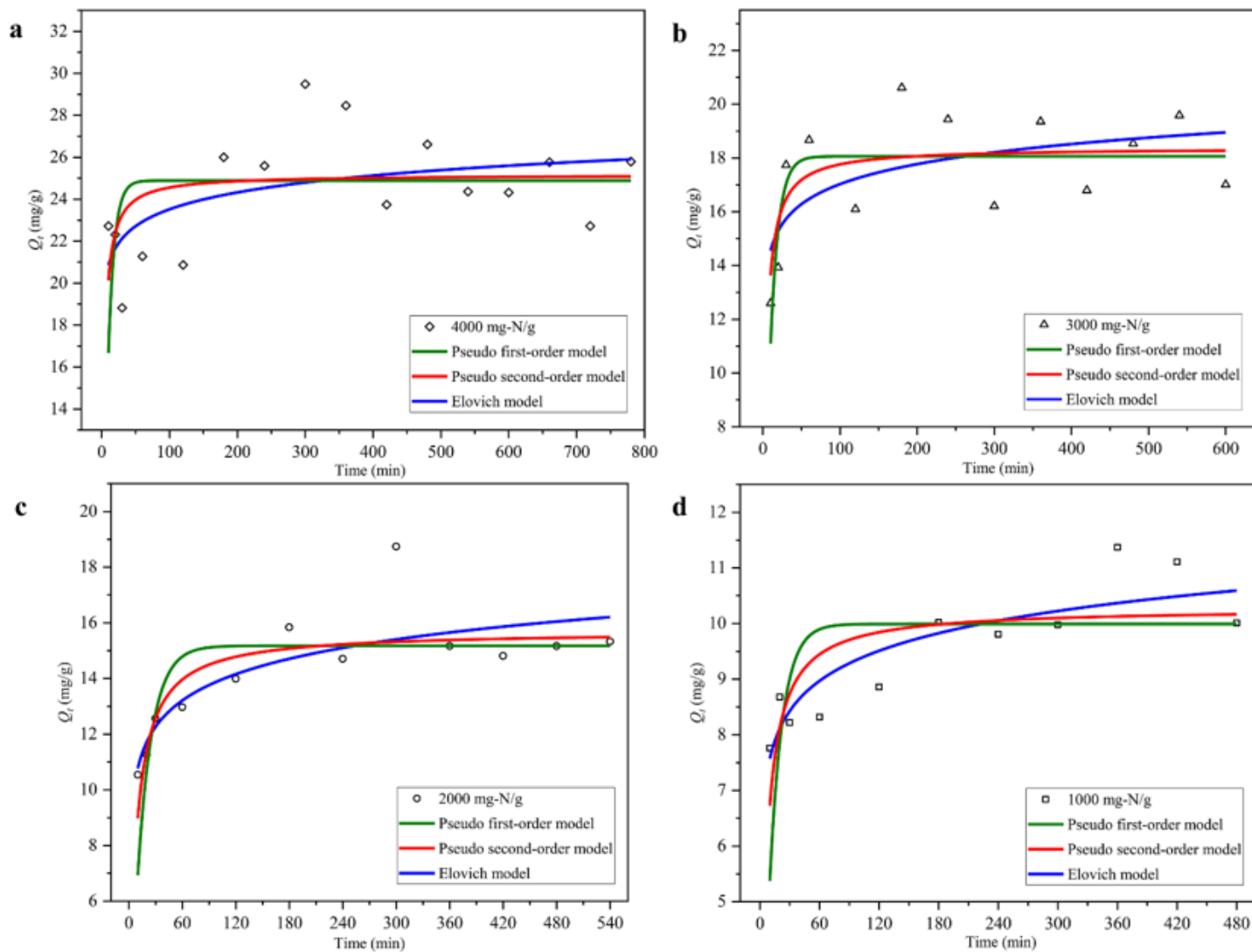


Figure 5

Nonlinear fitting of ammonium adsorption results with pseudo-first-order, pseudo-second-order and the intraparticle-diffusion model.

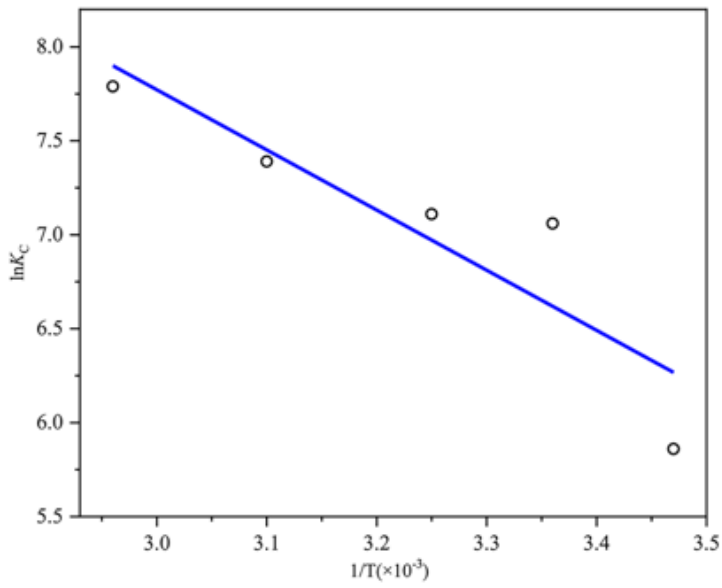


Figure 6

Fitting of the adsorption results of by the natural zeolite with the van't Hoff equation.

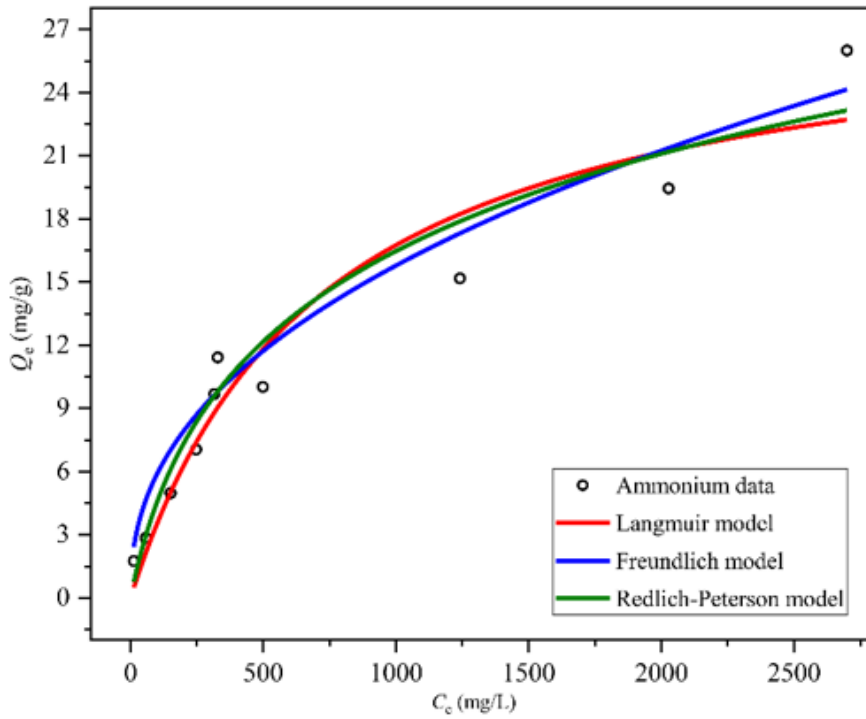


Figure 7

Nonlinear fitting of ammonium with Langmuir, Freundlich and Redlich-Peterson model.

Image not available with this version

Figure 8

Figure 8 was attributed to strong covalent linkage because the distance of the ammonium and framework oxygens was shortened by the electronic sharing between adsorbate and adsorbent.

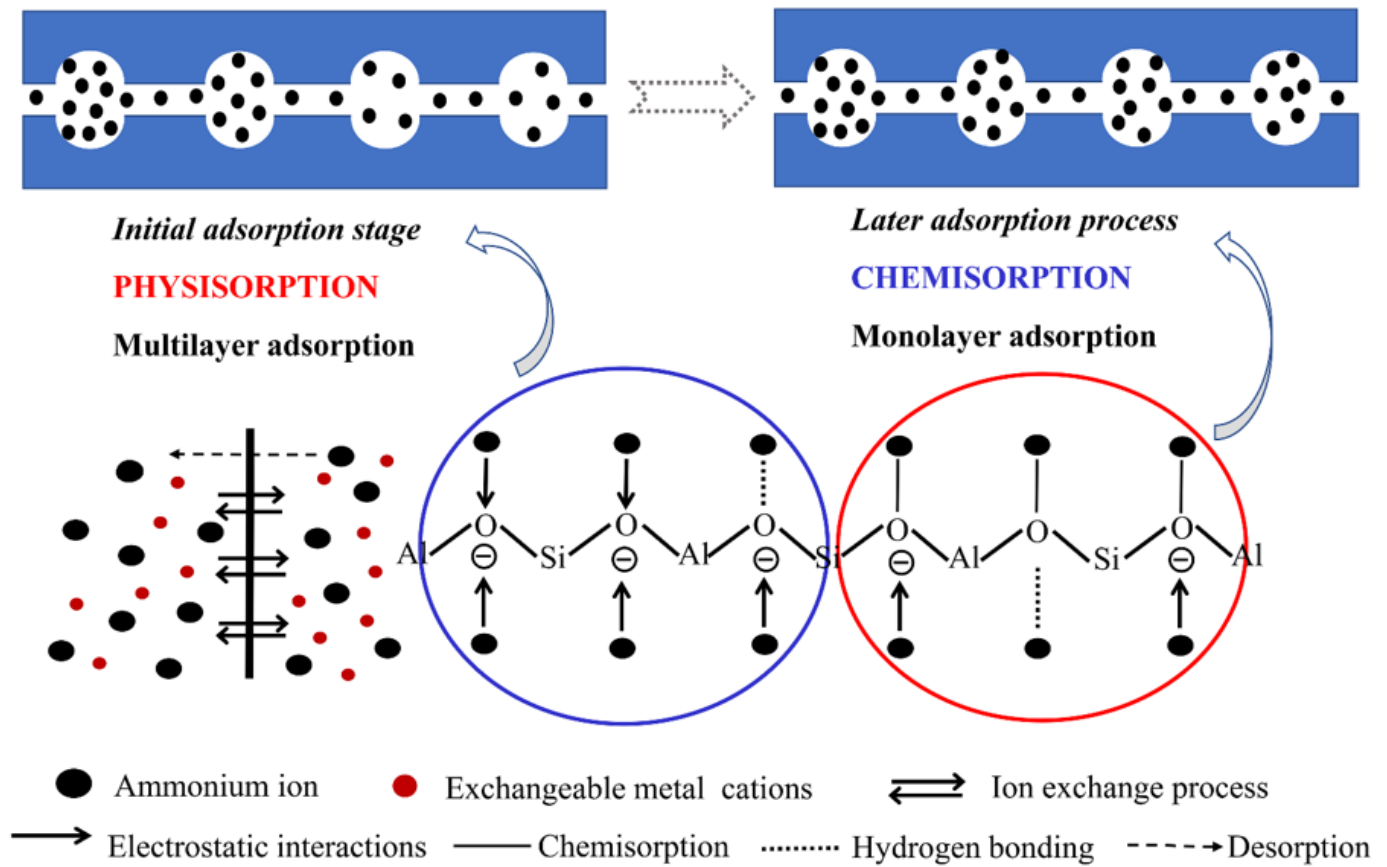


Figure 9

Schematic diagram for the adsorption mechanism of ammonium by the natural zeolite.

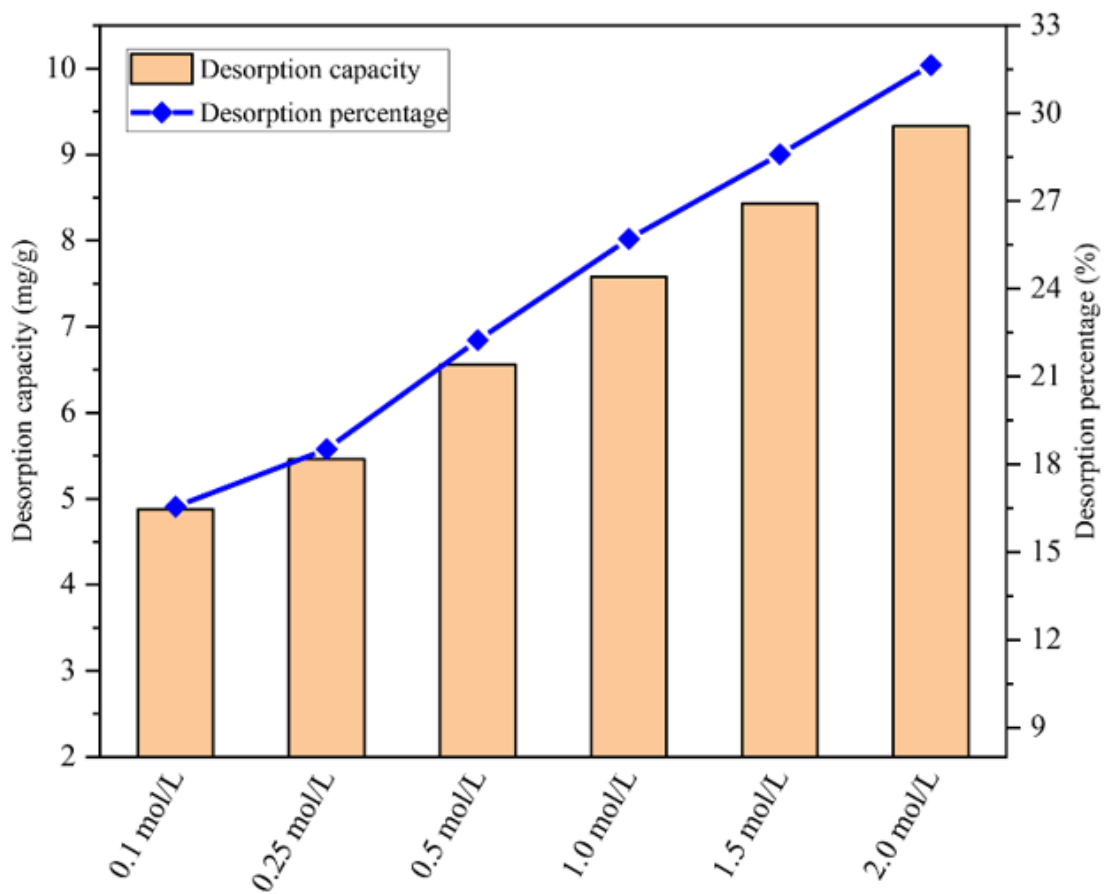


Figure 10

The zeolite regeneration in NaCl solution under different concentrations.

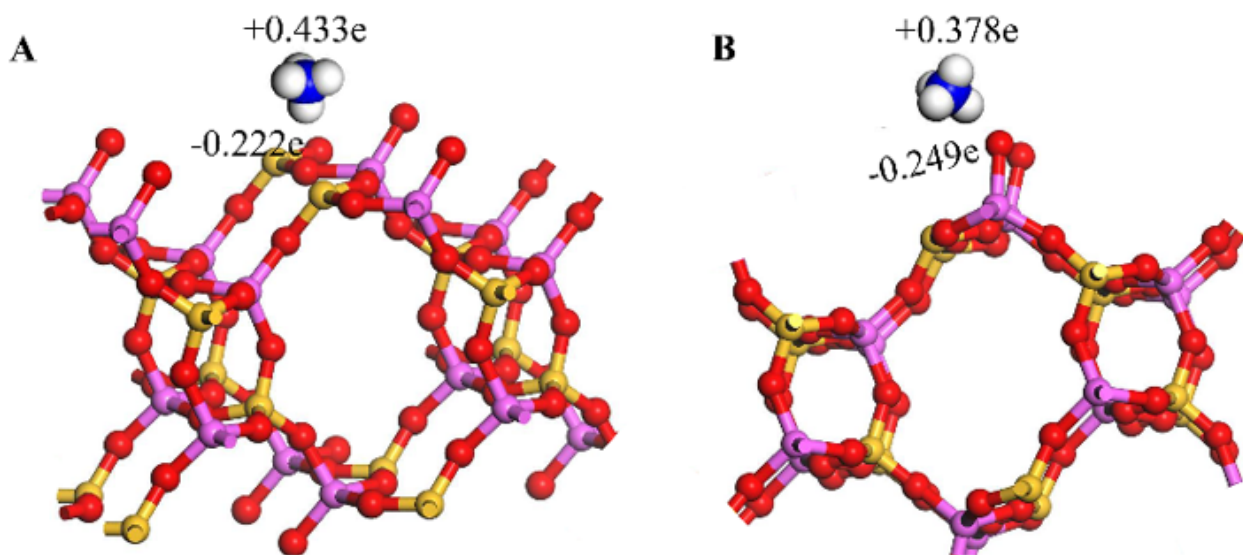


Figure 11

Visualization of Hirshfeld charges between ammonium and two types of O atom in the framework of natural zeolite. (A) on bridged O site, (B) on unbonded O site.

Supplementary Files

This is a list of supplementary files associated with this preprint. Click to download.

- [Supplementinformation.docx](#)